01,11

Calorimetry of eutectoid transformation in the Fe−C system

© L.V. Spivak[1], N.E. Shchepina[2]

[1] Perm State University,
Perm, Russia
[2] Institute of Natural Sciences of Perm State University,
Perm, Russia

E-mail: lspivak2@mail.ru

Received February 2, 2024
Revised May 24, 2024
Accepted May 25, 2024

The regularities of the manifestation of endothermic and exothermic effects during the transformations of perlite and austenite have been studied using differential scanning calorimetry. The enthalpy and entropy of eutectoid transformation at different heating and cooling rates were estimated by direct measurements. In particular, for a heating rate of 5 K/min $\Delta H = 2380$ J/mol and the entropy of such a transition is $\Delta S = 2.32$ J/(mol · K). It is suggested that in pre-eutectoid steels, when heated above the A_{C1} point (the critical point in the Fe−Cstate diagram when heated), the transition of perlite to austenite and the transition of excess ferrite to austenite occurs by its own set of mechanisms, each of which is realized at different temperatures in the intercritical (between points A_{C1} and A_{C3}) temperature range. An explanation of the independence of the temperature of the A_{C1} point from the carbon content in Fe−C alloys is proposed

Keywords: perlite, austenite, ferrite, phase.

DOI: 10.61011/PSS.2024.07.58979.17

1. Introduction

The phase diagrams (PD) of two and more components have several temperature-concentration points where using the Gibbs phase rule provides zero degree of freedom for the system$C$ ($C = k-f+1$, where k — number of components, f — number of phases in equilibrium, constant outer pressure), i. e. the so-called non-variant equilibrium. In particular, in Fe−C phase diagram these points include the temperature of polymorphic transformation $\alpha \leftrightarrow \gamma$ and temperature of eutectoid transformation perlite $\leftrightarrow$ austenite (carbon 0.8 wt%). In Fe−C phase diagram this temperature corresponds to point A_{C1} during heating and point A_{r1} during cooling.

The fact that non-variant equilibrium occurs in this point of the phase diagram is itself an evidence that the phase transformation shall be considered a first order phase transformation (PT-I). However, the phase diagram represents an idealized case that doesn't exist in real life. Apart from it, such thermodynamic approach doesn't allow considering possible mechanisms of such phase transformations.

In view of this, one of the tasks of this research was studying this transformation using other assessments (apart from Gibbs rule and dilatometry) of the phase transformation specifics when two phases from one phase are formed during cooling or one phase from two phases is formed during heating. For this purpose, the high-resolution differential scanning calorimetry (DSC) techniques were used.

The point, in particular, is what criteria of DSC data analysis can be a sufficient basis to consider one or another calorimetric effects at DSC as caused exactly by PT-I.

As early as in [1] it was shown for such a classic example of PT-I that total crystallization rate achieves its maximum almost exactly at the moment when crystallized volume achieves a half of the initial volume. This dependence of crystallization rate versus time passes through its maximum and is characterized by a symmetric nature.

Presuming that the thermal effect of transformation is proportional to the quantity of substance transforming to the new phase (see [2,3]), an extreme point should (and is) observed on the DSC signal curve in the region of phase transformation temperatures. And in the special cases, when the endothermic peak while heating can be approximated by close to Gaussian 2 functions, the maximum of this function is represented by the extreme point of DCS signal second derivative with respect to temperature.

When the difference between temperatures of extreme points of DSC signal curves and its second derivative is out of allowed errors of the experiment, we may consider, then, that these features of the DSC signal are either attributable to phase transformations realized not by one, as it was in the previous case, but by two or more mechanisms, or no any PT-I takes place at all in this temperature interval.

On the other hand, the phase transitions solid state → solid state, solid state → solid state + gas or solid state → liquid state during heating in terms of kinetics are often considered as some equivalent of chemical reaction [3–5], the general kinetic expression of which for the

solid-state reactions can be written as

$$\frac{d\alpha}{dt} = F(T)f(\alpha), \tag{1}$$

where $d\alpha/dt$ — reaction rate; $f(\alpha)$ — reaction kinetic function; $F(T)$ — effect of temperature T on the reaction rate.

It is known, that the function $f(\alpha)$ can be described by different equations, depending on the implementation mechanism proposed for the given process. For the solid state → solid state transformation implemented through emergence and growth of new phase nuclei, the Avrami–Erofeev [6] equation is used:

$$[-\lg(1-\alpha)]^{1/m} = kt, \tag{2}$$

where α — percentage of transformed substance, k — Avrami constant, t — time, m — characteristic of leading mechanism of the transformation process (Avrami index).

Thus, for example, Kissinger (see [7,8]) used the following equation to describe the process of solid state → solid state + gas dissociation

$$\frac{d\alpha}{dt} = A(1-\alpha)^n \exp\left(-\frac{Q}{RT}\right), \tag{3}$$

where A — is a constant, n — empirical parameter of reaction; R — gas constant; Q — energy of activation.

As a result he proposed an equation to determine the energy of activation Q in the following form

$$Q = -R\frac{d\ln\left(\frac{\beta}{T^2}\right)}{d\left(\frac{1}{T}\right)}, \tag{4}$$

where β — heating rate, T — temperature of the endothermic peak maximum, R — gas constant.

It is essential, that this equation is independent from the n order parameter n in equation (3). It seems, that it is this fact that is responsible for the frequent use of this relationship to determine the energy of activation for the processes implemented by mechanisms other than those of [7]. Moreover, other proposed methods to determine the energy of process activation from the DSC data in the vast majority of cases also use the above-mentioned relationship for the rate of a chemical reaction (see [2,3,8]).

The order of reaction n can be determined from the relationship presented in [5,7]

$$n = 1.26\sqrt{S}. \tag{5}$$

Here S — form-factor of the DSC curve in the region of temperatures of endothermic process recording: a ratio of tangents between the tangent lines in tripping points of the thermal effect experimental dependence.

Shapes of DTA [3] and DSC [4,5] curves were theoretically calculated for different mechanisms of phase transformation: diffusion, reaction at the phase interface, nuclei growth process. For the first two mechanisms of them the order of reaction is $n < 1$. taking into account the form factor. For the process controlled by nucleus growth $n > 1$. Here $d\alpha/dt$ goes through the maximum and represents itself a symmetrical curve ($S = 1$).

In this work an attempt is made to compare these two approaches to the DSC data obtained during studying the eutectoid transformation of perlite ↔ austenite.

2. Research procedure

The components content in steel was defined by chemical analysis and X-ray spectral method using MIRA3 Tescan electronic microscope. Steel Y8 was used with the following composition (wt%: 0.81 C; 0.28 Si; 0.31 Mn; 0.22 Ni; 0.03 S; 0.03 P; 0.17 Cr; 0.22 Cu).

The differential scanning calorimetry measurements were performed using STA „Jupiter“ 449 device by Netzsch. Heating and cooling were performed in argon environment 5, 10, 20 and 40 K/min in the argon environment (99.998% Ar). The gas flow rate was 25–30 ml/min. The weight of samples was within 180–210 mg.

The experimental DSC data, including determination of critical points temperatures, were processed using „Proteus Analyses“ and „Fityk“ package software. To reduce the effect of unpredictable factors on DSC the approximation of experimental dependence of DSC signals was made using polynomials of 6–8 power.

An experiment was carried out where for each heating degree the individual samples were used with the same thermal history: full annealing at 860°C.

3. Experimental results and discussion thereof

Figure 1 illustrates a typical nature of DSC signal variation under heating and cooling of the eutectoid steel. The endothermic effect under heating and exothermic effect

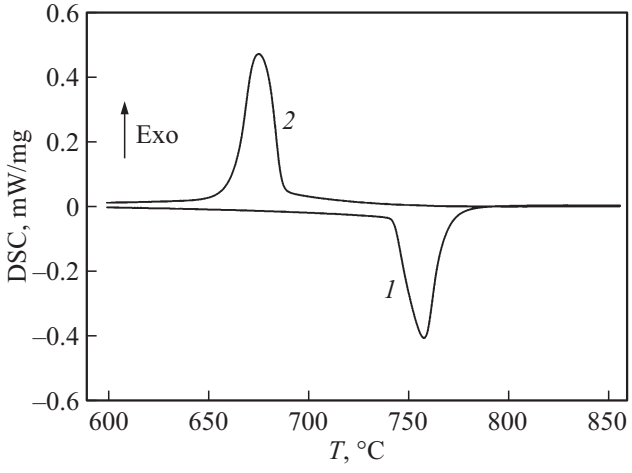

Figure 1. Variation of DSC signal during heating (curve *1*) and cooling (*2*) of steel Y8.

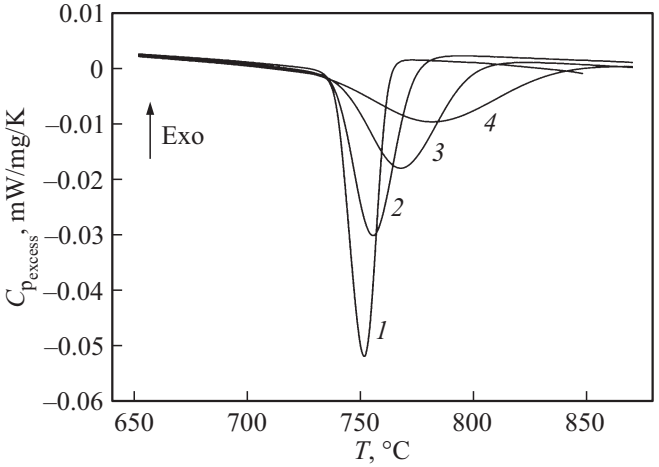

Figure 2. The effect of heating rates on the type and location of endothermic peaks during heating of Y8 steel: curve *1* — 5 K/min; *2* — 10 K/min; *3* — 20 K/min; *4* — 40 K/min. DSC signal value depending on the heating rate and sample weight was fixed on the *y*-axis.

under cooling is well approximated by the two near Gaussian relationships (e. g., SplitGaussian). Hysteresis between the onset temperature of transformation under heating and the onset temperature of transformation under cooling is observed. Within the specified range of thermal cycling rates such hysteresis didn't exceed 45–50°.

Figure 2 illustrates the effect of heating rate on DSC signal variation. On the *y*-axis the so-called reduced heat capacity $C_{p_{\text{excess}}}$ is plotted, which is the data of the DSC analysis normalized to the rate of heating (β) and weight (m_s) of samples (see [9]):

$$C_{p_{\text{excess}}} = \frac{\dot{Q}_S - \dot{Q}_{\text{Bl}}}{m_S \beta} \text{ J/(gK)}. \quad (6)$$

Here $\dot{Q}_S$ and $\dot{Q}_{\text{Bl}}$ — heat flow rates during heating of crucible with reference sample, respectively.

Proved by sufficiently high accuracy in this experiment, it may be said that the transformation onset temperature (see Figure 2) during heating practically is not influenced by the heating rate and is equal 740 ± 1°C. This feature is in line with the existing representations of the influence of the heating rate on the temperature of perlite transformation (A_{C1}) into austenite (see [10]).

However, the higher is the heating rate and temperatures the larger is both, the maximum displacement of the perlite-austenite transformation rate and the temperature of the process completion. For the temperature of endothermic effect (numerator) maximum and the temperature of second DSC-signal derivative maximum (denominator) within this temperature interval these temperatures are as follows: for heating rate 5, 10, 20 and 40 K/min — 752.5/752.9, 756.1/756.1, 767.1/767.1 and 780.2/780.9°C, respectively. Average temperature difference between the extreme points — 0.3°. Because of such small discrepancy between the temperatures of extreme points, we may (see [4,5]) consider this fact as one that proves that one and the same mechanism takes place in the transformation and it relates to PT-I.

Transformation temperature interval for the heating rate 5, 10, 20 and 40 K/min is equal 22, 34, 57 and 90°C respectively, and thermal effect of transformation — 42.1, 39.8, 37.1 and 35.0 J/g respectively.

With the increase of cooling rate (see Figure 3) the transformation onset temperature is slightly reduced. The maximum exothermic effect rate temperature is displaced notably towards the lower temperatures area and the perlite formation temperature is increased (see Figure 3). They are, respectively, equal: for the cooling rate 5, 10, and 20 K/min— 685.5/685.2, 17°C; 676.0/676.1, 27°C; 662.1/662.1, 40°C respectively; for the cooling rate 40 K/min— 693.5/693.4, 108°C. Average temperature difference between the extreme points — 0.3°.

Transformation thermal effect under cooling for 5, 10, 20 and 40 K/min— 55.0 J/g, 52.0 J/g, 52.0 J/g and 51.0 J/g respectively.

The displacement of maximum of the perlite-to-austenite transformation gives an opportunity, in particular, using Kissinger method [7], to assess the activation energy Q of this process from the formula (4).

Figure 4 illustrates the relationship between $\ln\left(\frac{\beta}{T_m^2}\right)$ and $1/T_m$.

The tangent of curves slope in these coordinates allows us to assess the process activation energy. For small heating rates $Q_1 = 1300 \pm 300$ kJ/g, and for higher heating rates $Q_2 = 500 \pm 100$ kJ/g.

Going back to determination of order parameters and considering perlite transformation as a kinetics of a chemical reaction, then, in our case, for the heating rates 5, 10, 20 and 40 K/min the average value $n = 1.20 \pm 0.03$. Hence,

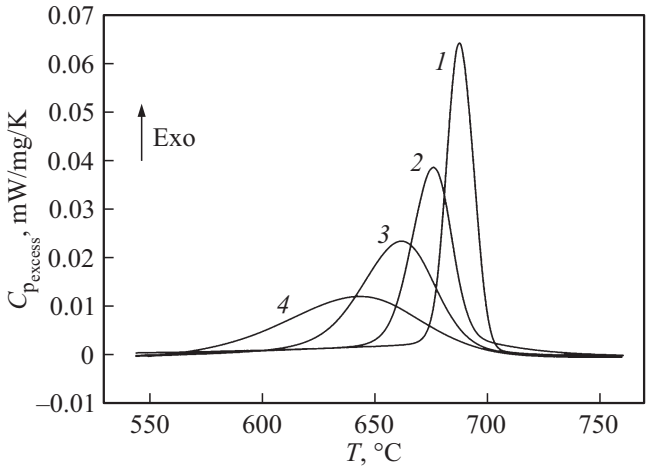

Figure 3. The effect of cooling rates on the type and location of exothermic peaks during cooling of Y8 steel: curve *1* — 5 K/min; *2* — 10 K/min; *3* — 20 K/min; *4* — 40 K/min. DSC signal value depending on the heating rate and sample weight was plotted on the *y*-axis.

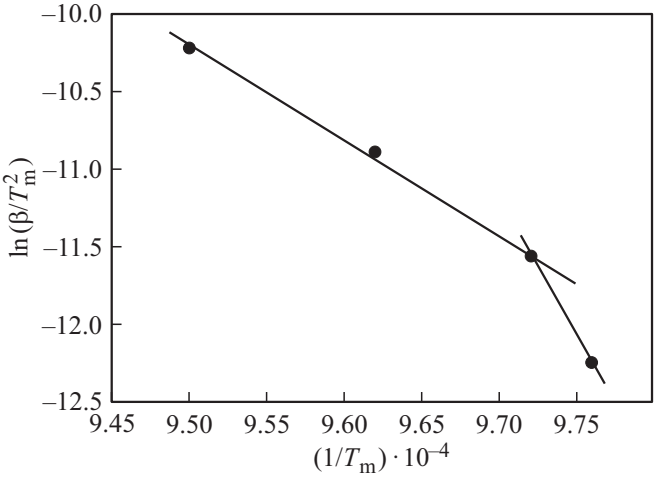

Figure 4. Relationship between the value $\ln(\beta/T_m^2)$ in Kissinger formula and the reverse temperature of the endothermic maximum $(1/T_m)$.

according to [3], it follows that during heating the process of perlite-to-austenite transformation can be controlled by observing the production and growth of austenite crystals.

The thermal effect of transformation, as seen from the obtained data, depends on the heating or cooling rates. This makes it a bit difficult to evaluate the enthalpy and entropy of the perlite $\leftrightarrow$ austenite transformation. Therefore, apparently, we shall focus on results obtained with the thermal cycling rate of 5 K/min, as the closest to the system equilibrium state. The molar weight calculated based on Y8 steel composition appeared to be equal to 56.57 g/mol. Thus, we have enthalpy of perlite $\rightarrow$ austenite transition as $\Delta H = 2380$ J/mol and the entropy of such transition is $\Delta S = 2.32$ J/(mol · K). During cooling these values are equal $\Delta H = 3110$ J/mol and $\Delta S = 3.25$ J/(mol · K), respectively.

Since entropy generally describes the extent of the system ordering, then, in these conditions of the experiment we see that austenite has better structure arrangement than perlite.

It is interesting to compare these data with equivalent data obtained from polymorphous transformation $\alpha \leftrightarrow \gamma$ of iron (see [11]). Average value of enthalpy of this phase transformation is $\Delta H = 280 \pm 25$ J/mol and for entropy $\Delta S = 0.24 \pm 0.02$ J/(mol · K). Energy activation of $\alpha \rightarrow \gamma$-transformation appeared to be equal 2300 ± 150 kJ/mol. Thus, this phase transition has a diffusionless nature (massive transformation) and relatively close value (low enthalpy value) of free energy level in α- and γ-states under the phase transition temperature.

Some patterns found in this paper shall be analyzed. The first of them is that thermal effect during heating (endothermic) is always slightly lower than the thermal effect (exothermic) which takes place during cooling. The reason of this, apparently, is that thermodynamic stimulus of transformation and diffusion activity of atoms during heating are unidirectional and increasing, while during cooling the thermodynamic stimulus of the transformation is growing, and diffusion activity of atoms is going down. A similar pattern can be seen during polymorphous transformation of pure iron [11].

In respect to our research object, among other things, during heating and cooling processes various phase transformation mechanisms take place. Figure 4 illustrates the perlite-to-austenite transition activation energy represented as a process occurring through the two mechanisms with their own activation energy values. At relatively small heating rates (small thermodynamic transformation stimulus) the mechanisms with high activation energies of phase transformation take place. The latter are characteristic for the diffusionless transformation mechanisms. In particular, in [12] the appearance of austenite nucleus is deemed as a diffusion-less shear like mechanism. The activation energy below 800 kJ/mol indicates that mainly diffusion mechanisms are responsible for the perlite-to-austenite transition (growth of the austenite nucleus).

Thus, perlite $\leftrightarrow$ austenite transformation has the same manifestations as the polymorphous transformation $\alpha \leftrightarrow \gamma$ in iron. Both of the transformations are PT-I but occurring through different mechanisms as seen in the major iron–carbon diagram.

In description of the transformation structural pattern for the hypoeutectic steels it is usually interpreted as a growth of austenite nucleus into ferrite (see [12–14]). However, in terms of thermodynamics this process is a transition of ferrite (less thermodynamic equilibrium state) into austenite (more thermodynamic equilibrium state). It seems that during austenitization of hypoeutectic steels the processes of austenite formation from perlite and austenite formation from proeutectoid ferrite go separately (see, for instance [15]).

It appeared that specific values of thermal effects and their temperatures recorded during the eutectoid transformation depend on the thermal history of the material. This can be considered as another example of manifestation called „structural-phase heredity“ (see [16]) with its specifics and individual process peculiarities.

The patterns identified in perlite $\leftrightarrow$ austenite transformations, appear to occur to some extent during eutectoid transformations in alloys also with other phase diagrams, different from Fe–C.

4. Conclusion

For the first time the direct measurements allowed to determine the enthalpy and entropy of direct and reverse transformation of perlite $\leftrightarrow$ austenite with various heating and cooling rates.

The results of determining the activation energy of perlite $\leftrightarrow$ austenite transition indicate that there are two stages of the transition: diffusion-less and diffusion stages.

Since perlite $\leftrightarrow$ austenite transition is PT-I, its is presumed that two stages of austenite formation shall take place when

heating the hypoeutectic steels above A_{C1}. The first stage is related to perlite-to-austenite transition. The second stage is related to austenite transition to proeutectoid ferrite.

The concept of „structural-phase heredity“ was broadened in view of the calorimetric effects dependence during the thermal cycling of alloys on their thermal history.

The obtained research results may serve as a proof that the point (line) A_{C1} in Fe−C phase diagram doesn't depend on the carbon content in Fe−C alloy. Mandatory condition — availability of perlite in the alloy. The perlite-to-austenite transition looks like a shear phase transformation, therefore, the heating rate, as demonstrated and proved in this paper, has poor effect on the temperature of point A_{C1} in Fe−C phase diagram.

Conflict of interest

The authors declare that they have no conflict of interest.

References

[1] A.K. Kolmogorov. Izv. AN SSSR. Ser. matem. **1**, *3*, 355 (1937).
[2] W.W. Wendlandt. Thermal Methods of Analysis. 2nd ed. John Wiley & Sons (1974). 505 p.
[3] J. Šesták. Thermophysical Properties of Solids. Measurments. Their Theoretical Thermal Analysis. Academia Prague (1984). 456 p.
[4] A.K. Galwey, M.E. Brown. Handbook of Thermal Analysis and Calorimetry. V. **1**: Principles and Practice / Ed. M.E. Brown. Elsevier Science B.V. (1998). 147 p.
[5] Introduction to thermal analysis / Ed. M.E. Brown. Kliwer Academic Publishers. N.Y., Boston, Dordricht, London, Moscow (2001). 264 p.
[6] M. Avrami. J. Chem. Phys. **7**, *12*, 1103 (1939). https://doi.org/10.1063/1.1750380.
[7] H.E. Kissinger. Anal. Chem. **29**, *11*, 1702 (1957). https://doi.org/10.1021/ac60131a045
[8] S. Vyazovkin, A.K. Burnham, J.M. Criado, L.A. Pérez-Maqueda, C. Popescu, N. Sbirrazzuoli. Thermochim. Acta **520**, *1–2*, 1 (2011). https://doi.org/10.1016/j.tca.2011.03.034
[9] S.M. Sarge, G.W.H. Höhne, W.F. Hemminger. Calorimetry: Fundamentals, Instrumentation and Applications. Wiley-VCH Verlag GmbH & Co. KGaA: Weinheim, Germany (2014). 280 p.
[10] S.V. Grachev. Fizicheskoe metallovedenie: uchebnik dlya vuzov / Pod. red. S.V. Grachev, V.R. Baraz, A.A. ogatov, V.P. Shveikin Izd-vo Uralskogo gos.un-ta, UPI, Ekaterinburg (2001). 534 p. (In Russian).
[11] L.V. Spivak, N.E. Shchepina. Tech. Phys. **65**, *7*, 1100 (2020).
[12] S.S. Diachenko. Obrazovanie austenita v zhelezouglerodistykh splavakh. Metallurgiya, M., (1982). 128 p. (in Russian).
[13] V.I. Zel'dovich. Metal Sci. Heat Treatment **50**, *9–10*, 442 (2008).
[14] D.O. Panov, A.I. Smirnov. Phys. Metals. Metallogr. **118**, *11*, 1073 (2017).
[15] L.V. Spivak, N.E. Schepina. Metally **1**, 1 (2024). (in Russian).
[16] S.S. Diachenko. MiTOM *4*, 14 (2000). (in Russian).

Translated by T.Zorina